

Supporting Information for

**Work Function Regulation of Surface-engineered Ti₂CT₂ MXene for
Efficient Electrochemical Nitrogen Reduction Reaction**

Yaqin Zhang^a, Ninggui Ma^a, Tairan Wang^a, Jun Fan^{a,b,c}*

^a *Department of Materials Science and Engineering, City University of Hong Kong,
Hong Kong, China*

^b *Center for Advanced Nuclear Safety and Sustainable Development, City University of
Hong Kong, Hong Kong, China*

^c *Department of Mechanical Engineering, City University of Hong Kong, Hong Kong,
China*

* *Corresponding author. E-mail: junfan@cityu.edu.hk (Jun Fan)*

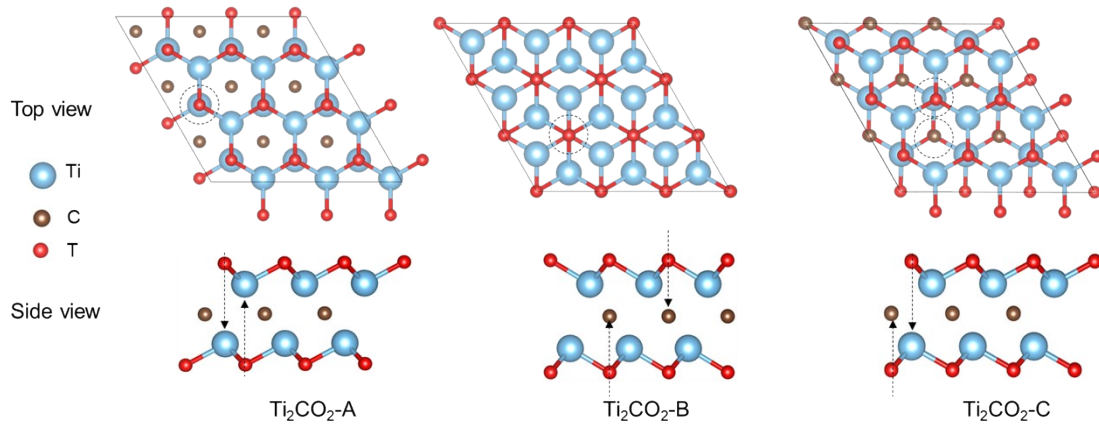


Fig. S1 Configurations of Ti_2CT_2 models

Table S1 Total electronic energy of supercell (E_0), unit cell (E_b), formation energy (E_f), and defect formation energy (E_{def}). Formation energy for Ti_2CT_2 MXene: $E_f = (E_0 - E_{\text{Ti}_2\text{C}} - x \times E_{\text{T}})/x$. Defect formation energy is only considered for the most stable one among the three configurations: $E_{\text{def}} = E_{\text{Ti}_2\text{CT}_2-\text{V}} - E_{\text{Ti}_2\text{CT}_2} + E_{\text{T}}$.

Ti_2CT_2	E_0 (eV)	E_b (eV)	E_f (eV)	E_{def} (eV)
$\text{Ti}_2\text{CF}_2\text{-A}$	-354.42	-115.71	-6.81	6.60
$\text{Ti}_2\text{CF}_2\text{-B}$	-349.92	-111.21	-6.54	NA
$\text{Ti}_2\text{CF}_2\text{-C}$	-352.57	-113.86	-6.70	NA
$\text{Ti}_2\text{CH}_2\text{-A}$	-311.14	-63.92	-3.76	3.69
$\text{Ti}_2\text{CH}_2\text{-B}$	-305.26	-58.04	-3.41	NA
$\text{Ti}_2\text{CH}_2\text{-C}$	-307.87	-60.65	-3.57	NA
$\text{Ti}_2\text{CO}_2\text{-A}$	-402.17	-141.61	-8.33	7.59
$\text{Ti}_2\text{CO}_2\text{-B}$	-388.23	-127.66	-7.51	NA
$\text{Ti}_2\text{CO}_2\text{-C}$	-395.76	-135.19	-7.95	NA
$\text{Ti}_2\text{COH}_2\text{-A}$	-457.10	-101.90	-5.99	5.39
$\text{Ti}_2\text{COH}_2\text{-B}$	-454.37	-99.17	-5.83	NA
$\text{Ti}_2\text{COH}_2\text{-C}$	-456.04	-100.84	-5.93	NA

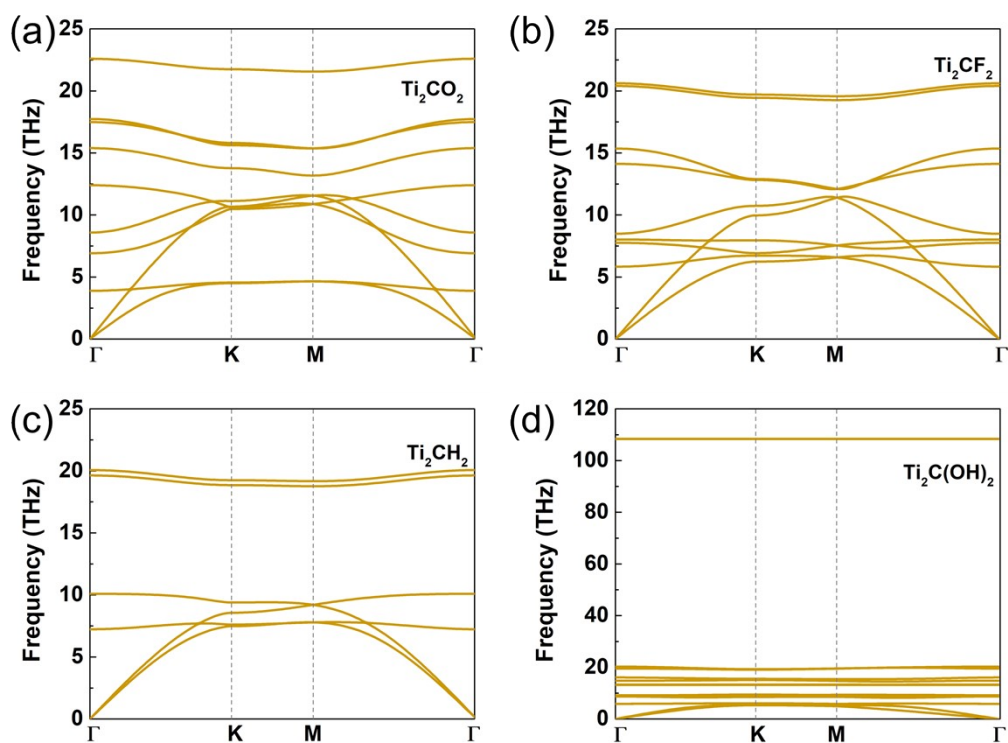


Fig. S2 Calculated phonon band structures of the Ti_2CT_2 unitcell.

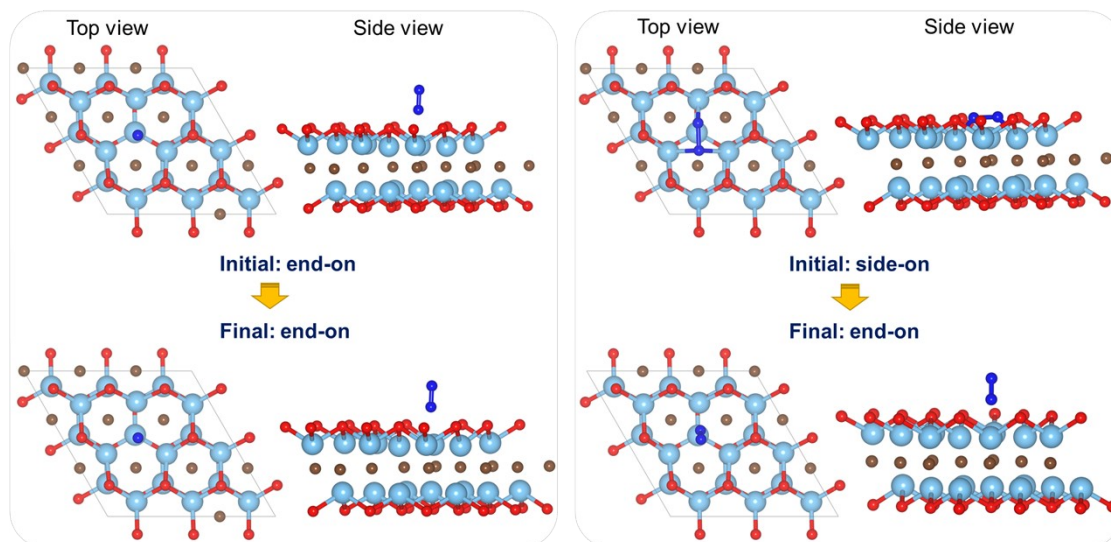


Fig. S3 The initial configurations of end-on and side-on adsorption and their optimized final states.

Table S2 Gibbs free energy through distal and consecutive mechanism

ΔG (distal)	Ti₂CO₂	Ti₂CF₂	Ti₂CH₂	Ti₂C(OH)₂
Slab	0.00	0.00	0.00	0.00
*N ₂	-0.03	-0.33	-0.39	-0.76
*NNH	0.50	-0.52	-0.65	-1.11
*NNH ₂	-0.72	-1.21	-1.59	-1.14
*N	-0.97	-2.10	-2.10	-2.36
*NH	-2.06	-2.86	-2.90	-2.75
*NH ₂	-2.02	-2.48	-2.56	-2.08
*NH ₃	-1.90	-1.58	-1.36	-0.79
slab	-0.89	-0.89	-0.89	-0.89
ΔG (consecutive)	Ti₂CO₂	Ti₂CF₂	Ti₂CH₂	Ti₂C(OH)₂
Slab	0.00	0.00	0.00	0.00
*N ₂	-0.03	-0.33	-0.39	-0.76
*NNH	0.50	-0.52	-0.65	-1.11
*NH-NH	0.00	-0.84	-1.11	-0.20
*NH-NH ₂	-0.53	-0.99	-1.27	-0.09
*NH ₂ -NH ₂	-0.12	0.15	0.27	1.33
*NH ₂	-2.02	-2.48	-2.56	-2.08
*NH ₃	-1.90	-1.58	-1.36	-0.79
slab	-0.89	-0.89	-0.89	-0.89

Table S3 Free energy barrier through distal and consecutive mechanism including electronic steps.

ΔG (distal)	Ti₂CO₂	Ti₂CF₂	Ti₂CH₂	Ti₂C(OH)₂
*N ₂	NA	NA	NA	NA
*NNH	0.53	-0.19	-0.27	-0.35
*NNH ₂	-1.22	-0.69	-0.94	-0.03
*N	-0.24	-0.90	-0.51	-1.21
*NH	-1.10	-0.75	-0.80	-0.40
*NH ₂	0.04	0.38	0.34	0.67
*NH ₃	0.12	0.90	1.21	1.29
ΔG (consecutive)	Ti₂CO₂	Ti₂CF₂	Ti₂CH₂	Ti₂C(OH)₂
*N ₂	NA	NA	NA	NA
*NNH	0.53	-0.19	-0.27	-0.35
*NH-NH	-0.50	-0.32	-0.45	0.92
*NH-NH ₂	-0.53	-0.15	-0.17	0.10
*NH ₂ -NH ₂	0.41	1.15	1.54	1.42
*NH ₂	-1.90	-2.63	-2.83	-3.41
*NH ₃	0.12	0.90	1.21	1.29

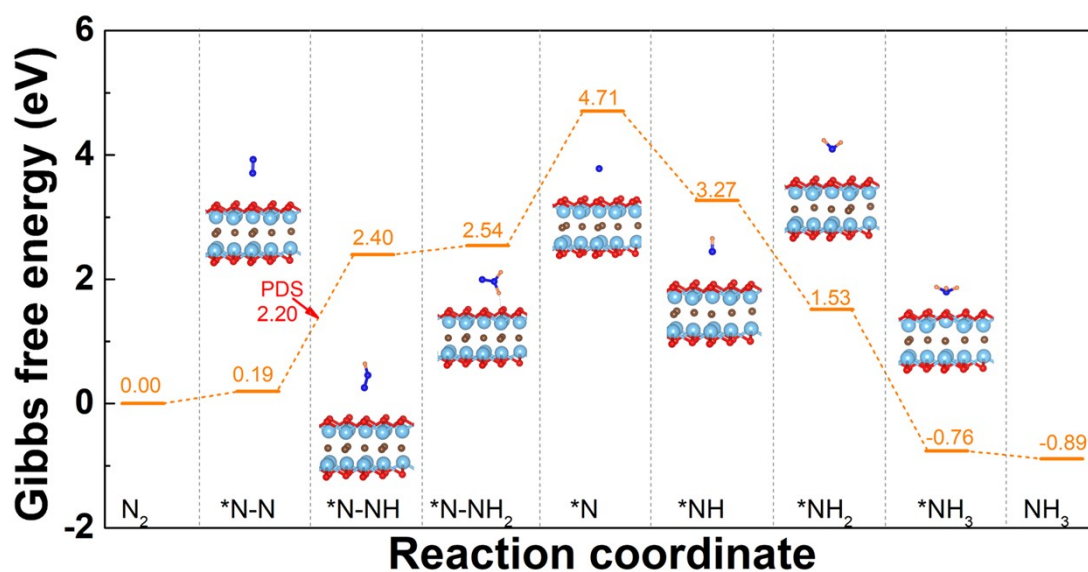


Fig. S4 Free energy profiles for nitrogen reduction on perfect Ti_2CO_2 through distal mechanisms, and the configuration for each reaction intermediate is shown as well.

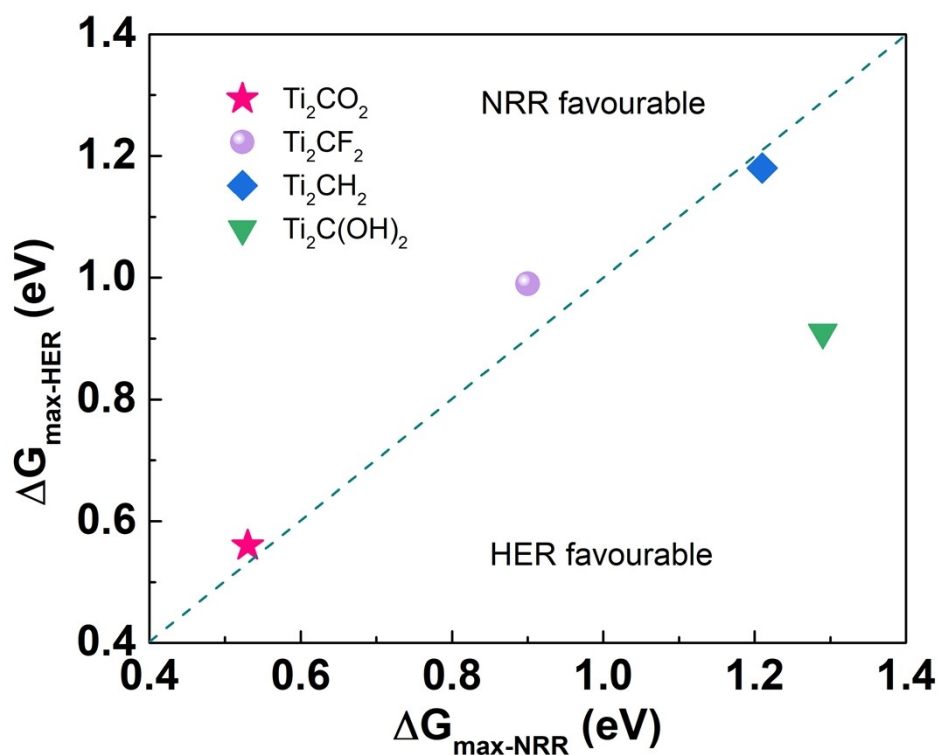


Fig. S5 Free energy potential of rate-determining steps for NRR and HER. The values of ΔG_{max} for HER are 0.56 eV (Ti_2CO_2), 0.99 eV (Ti_2CF_2), 1.18 eV (Ti_2CH_2), and 0.91 eV ($\text{Ti}_2\text{C}(\text{OH})_2$). The dashed line represents $\Delta G_{\text{max-HER}} = \Delta G_{\text{max-NRR}}$.

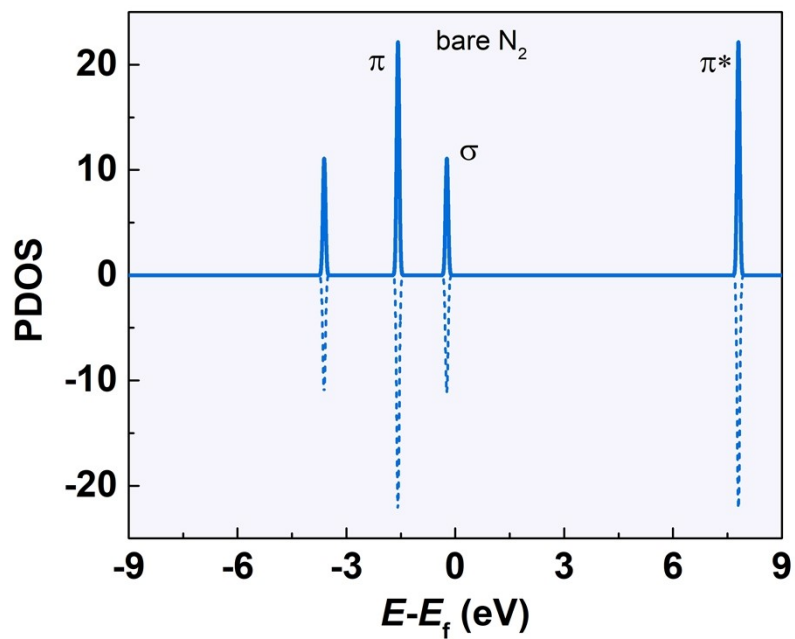


Fig. S6 Projected density of states of pure N_2 molecule.

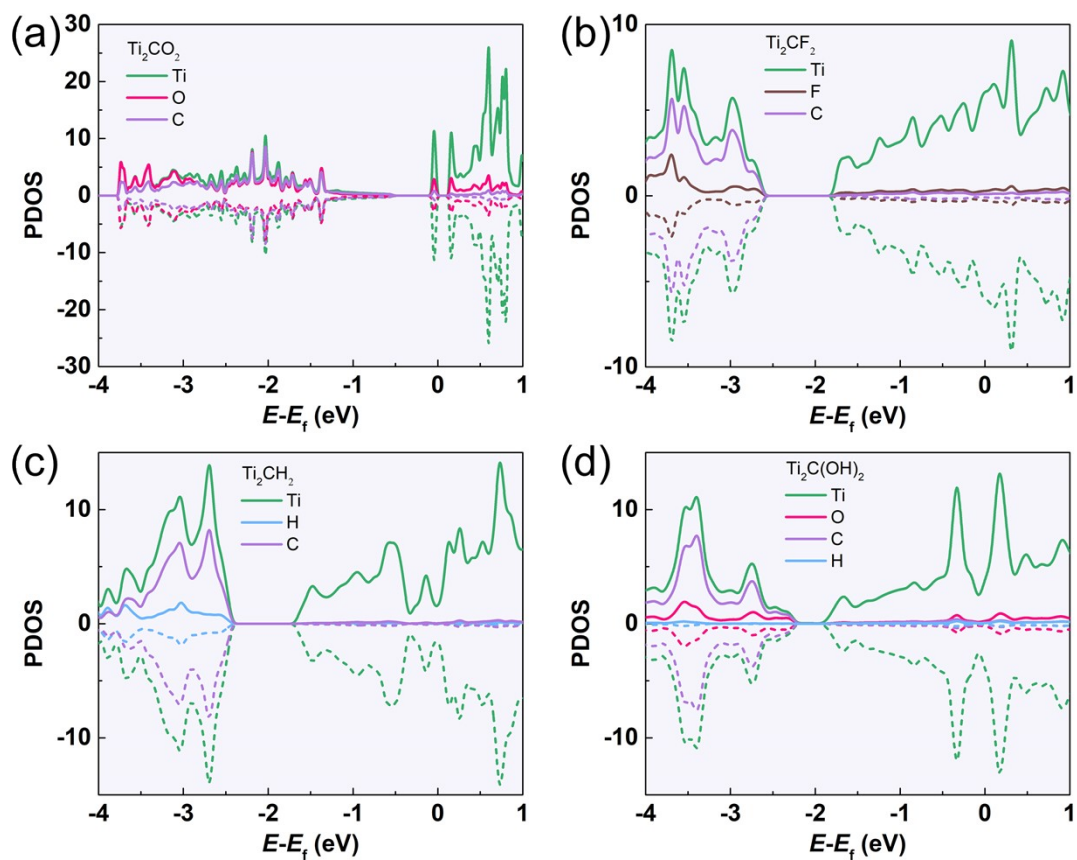


Fig. S7 Projected density of states of defective (a) Ti_2CO_2 , (b) Ti_2CF_2 , (c) Ti_2CH_2 , and (d) $Ti_2C(OH)_2$.

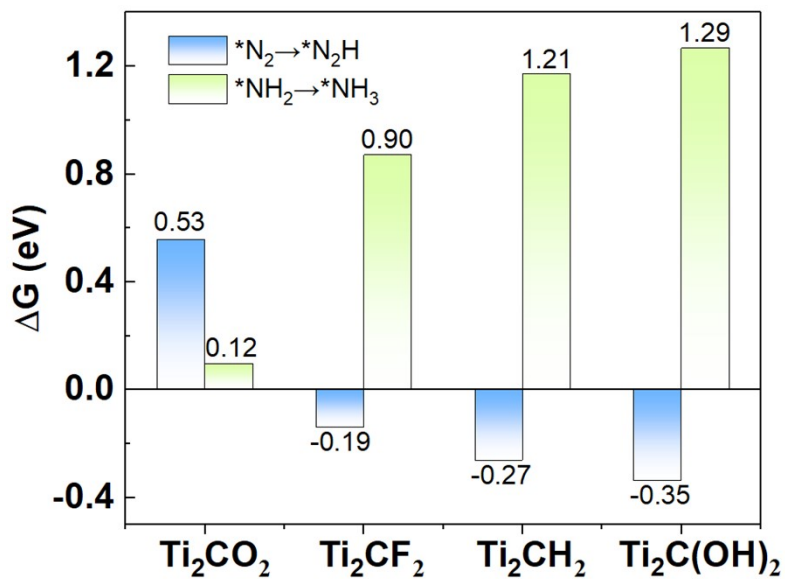


Fig. S8 Free energy barrier of potential-determining steps following distal path.

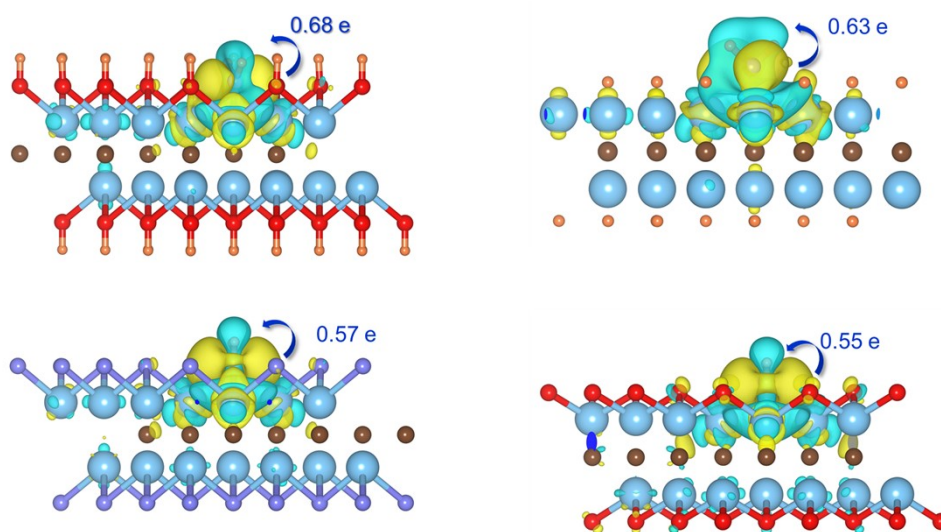


Fig. S9 Charge transfer and electron density difference between defective (a) Ti₂C(OH)₂, (b) Ti₂CH₂, (c) Ti₂CF₂, and (d) Ti₂CO₂ and intermediate *NH₂.

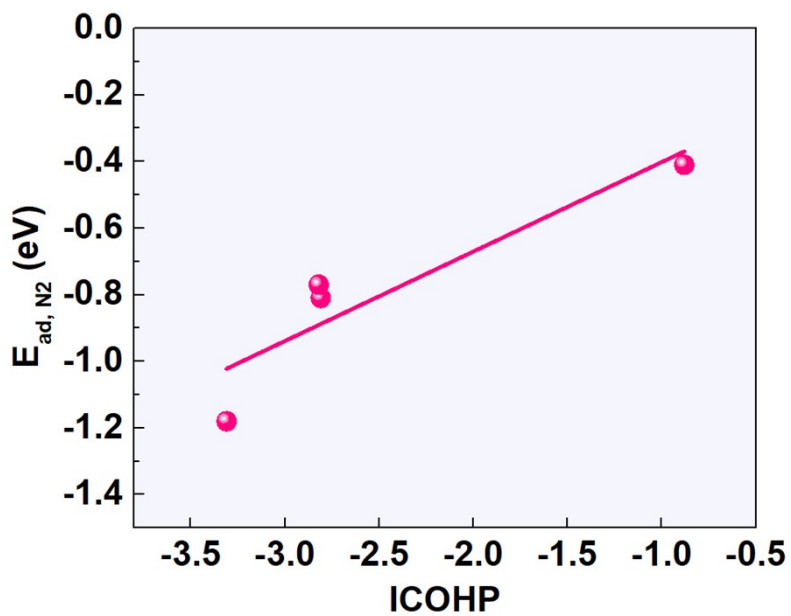


Fig. S10 Linear fitting between ICOHP and adsorption energy of N₂.

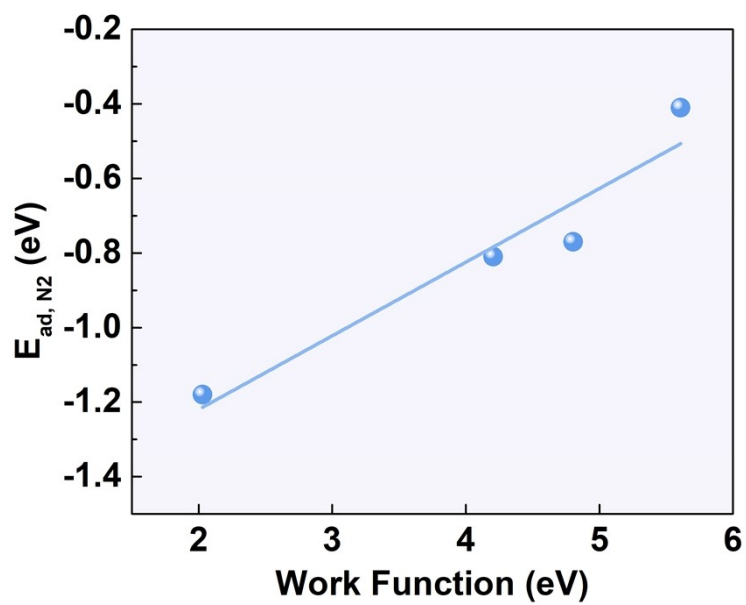


Fig. S11 Linear fitting between work function and adsorption energy of N₂.